J|A|C|S

A R T I C L E S

Conservation of Mechanism in Three Chorismate-Utilizing Enzymes

Ze He,[†] Kimberly D. Stigers Lavoie,[‡] Paul A. Bartlett,[‡] and Michael D. Toney[*,†]

*Contribution from the Department of Chemistry, University of California-Davis,
Davis, California 95616, and Department of Chemistry, University of California-Berkeley,
Berkeley, California 94720*

Received October 10, 2003; E-mail: mdtoney@ucdavis.edu

Abstract: Chorismate is the end-product of the shikimate pathway for biosynthesis of carbocyclic aromatic compounds in plants, bacteria, fungi, and some parasites. Anthranilate synthase (AS), 4-amino-4-deoxychorismate synthase (ADCS), and isochorismate synthase (IS) are homologous enzymes that carry out the initial transformations on chorismate in the biosynthesis of tryptophan, *p*-aminobenzoate, and enterobactin, respectively, and are expected to share a common mechanism. Poor binding to ADCS of two potential transition state analogues for addition of a nucleophile to C6 of chorismate implies that it, like AS and IS, initiates reaction by addition of a nucleophile to C2. Molecular modeling based on the X-ray structures of AS and ADCS suggests that the active site residue K274 is the nucleophile employed by ADCS to initiate the reaction, forming a covalent intermediate. The K274A and K274R mutants were shown to have 265- and 640-fold reduced k_{cat} values when PabA (the cognate amidotransferase) + glutamine are used as the nitrogen source. Under conditions of saturating chorismate and NH_4^+, ADCS and the K274A mutant have identical k_{cat} values, suggesting the participation of NH_4^+ as a rescue agent. Such participation was confirmed by the buildup of 2-amino-2-deoxyisochorismate in the reactions of the K274A mutant but not ADCS, when either NH_4^+ or PabA + glutamine is used as the nitrogen source. Additionally, the inclusion of ethylamine in the reactions of K274A yields the *N*-ethyl derivative of 2-amino-2-deoxyisochorismate. A unifying mechanism for AS, ADCS, and IS entailing nucleophile addition to C2 of chorismate in an S_N2'' process is proposed.

Introduction

The shikimate biosynthetic pathway (Figure 1) is found in plants, bacteria, fungi, and apicomplexan parasites.[1] It is central to the biosyntheses of a variety of carbocyclic aromatic compounds. The final product of the shikimate pathway, chorismate, is the branchpoint for the production of folate, aromatic amino acids, vitamins K and E, coenzyme Q, enterobactin, chloramphenicol, plastoquinones, phenoxazinones, and other metabolites. Some intermediates in these pathways also have important physiological roles. For example, salicylate is involved in plant defense against pathogens,[2] and anthranilate is the precursor to the *Pseudomonas* quinolone signal that is involved in virulence factor regulation in *Pseudomonas aeruginosa*.[3] The central importance of the chorismate-dependent pathways and their absence in mammals make them very attractive targets for the development of antimicrobials and herbicides.

Five common chorismate utilizing enzymes have been characterized. These include anthranilate synthase (AS),[4] 4-amino-4-deoxychorismate synthase (ADCS),[5] isochorismate synthase (IS),[6] chorismate mutase,[7] and chorismate lyase.[8] The first three of these enzymes possess high sequence homology and the X-ray structures of two of them, AS[9−11] and ADCS,[12] are very similar. This correlation is not surprising given the similarities of the reactions they catalyze. However, they also display interesting differences. For example, AS forms 2-amino-2-deoxyisochorismate (ADIC) as an enzyme-bound intermediate and subsequently catalyzes the elimination of pyruvate to form anthranilate in a single active site.[13,14] ADCS[15] and IS,[6] on the

† University of California-Davis.
‡ University of California-Berkeley.
(1) Roberts, C. W.; Roberts, F.; Lyons, R. E.; Kirisits, M. J.; Mui, E. J.; Finnerty, J.; Johnson, J. J.; Ferguson, D. J.; Coggins, J. R.; Krell, T.; Coombs, G. H.; Milhous, W. K.; Kyle, D. E.; Tzipori, S.; Barnwell, J.; Dame, J. B.; Carlton, J.; McLeod, R. *J. Infect. Dis.* **2002**, *185* (Suppl. 1), S25−36.
(2) Shah, J. *Curr. Opin. Plant Biol.* **2003**, *6*, 365−371.
(3) Calfee, M. W.; Coleman, J. P.; Pesci, E. C. *Proc. Natl. Acad. Sci. U.S.A.* **2001**, *98*, 11633−7.
(4) Romero, R. M.; Roberts, M. F.; Phillipson, J. D. *Phytochemistry* **1995**, *39*, 263−276.
(5) Viswanathan, V. K.; Green, J. M.; Nichols, B. P. *J. Bacteriol.* **1995**, *177*, 5918−5923.
(6) Liu, J.; Quinn, N.; Berchtold, G. A.; Walsh, C. T. *Biochemistry* **1990**, *29*, 1417−25.
(7) Davidson, B. E. *Methods Enzymol.* **1987**, *142*, 432−9.
(8) Holden, M. J.; Mayhew, M. P.; Gallagher, D. T.; Vilker, V. L. *Biochim. Biophys. Acta* **2002**, *1594*, 160−7.
(9) Spraggon, G.; Kim, C.; Nguyen-Huu, X.; Yee, M. C.; Yanofsky, C.; Mills, S. E. *Proc. Natl. Acad. Sci. U.S.A.* **2001**, *98*, 6021−6026.
(10) Morollo, A. A.; Eck, M. J. *Nat. Struct. Biol.* **2001**, *8*, 243−247.
(11) Knochel, T.; Ivens, A.; Hester, G.; Gonzalez, A.; Bauerle, R.; Wilmanns, M.; Kirschner, K.; Jansonius, J. N. *Proc. Natl. Acad. Sci. U.S.A.* **1999**, *96*, 9479−9484.
(12) Parsons, J. F.; Jensen, P. Y.; Pachikara, A. S.; Howard, A. J.; Eisenstein, E.; Ladner, J. E. *Biochemistry* **2002**, *41*, 2198−2208.
(13) Morollo, A. A.; Bauerle, R. *Proc. Natl. Acad. Sci. U.S.A.* **1993**, *90*, 9983−9987.
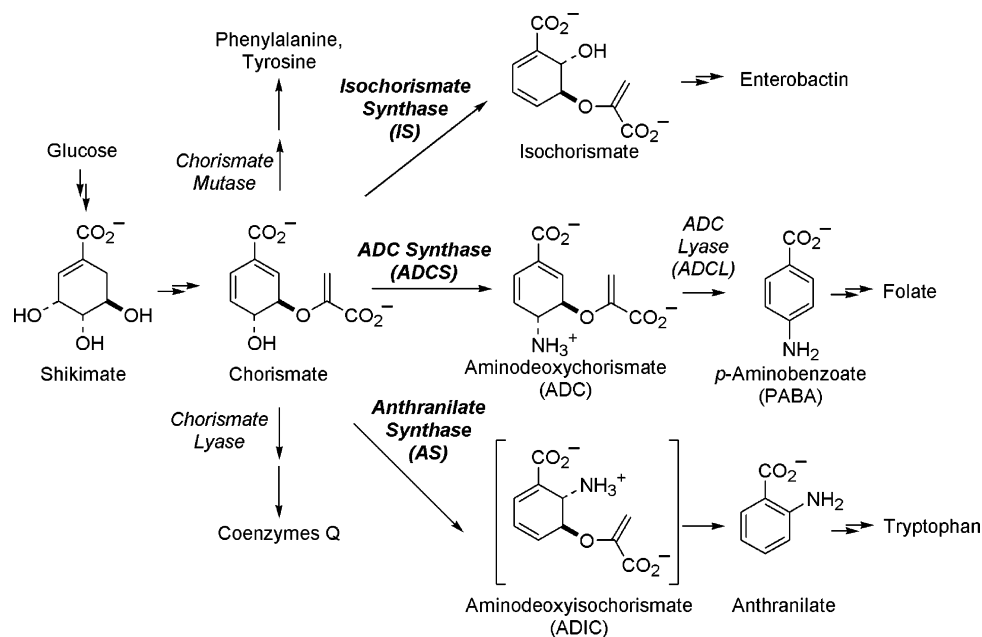
Figure 1. Overview of the chorismate pathway. Anthranilate synthase (AS), aminodeoxychorismate synthase (ADCS), and isochorismate synthase (IS) have strong sequence homology. The known structures of AS and ADCS are very similar.

other hand, do not eliminate pyruvate from the substituted chorismate products. It is interesting that ADCS does not do so, since elimination is the next step in the biosynthesis of *p*-aminobenzoic acid (PABA), catalyzed by 4-amino-4-deoxychorismate lyase (ADCL).

AS, IS, and ADCS catalyze replacement of the C4 hydroxyl group of chorismate with nitrogen (AS and ADCS) or oxygen (IS) nucleophiles. The reactions catalyzed by AS and IS involve nucleophilic addition to C2 of chorismate, replacing the original C4 hydroxyl group (chorismate ring numbering given in Figure 8). The displacement reaction of ADCS is more complex. In the final product, 4-amino-4-deoxychorismate (ADC), the C4 hydroxyl group of chorismate is replaced by an amino group with retention of the original stereochemistry.[16] The AS and IS reactions can, in principle, occur via a single S_N2''-type displacement reaction. In contrast, the ADCS reaction cannot occur via a single S_N2 displacement, since this mechanism would lead to inversion of stereochemistry. A variety of alternative mechanisms for ADCS have been proposed and tested, but the available evidence does not distinguish between them.[17]

Four mechanisms for AS, IS, and ADCS have been considered previously: (1) a Michael addition/elimination sequence with the formation of an aci-carboxylate intermediate; (2) addition of an enzyme active site nucleophile to C6 of chorismate; (3) covalent catalysis by the substrate itself in which the enoylpyruvate side chain carboxylate adds to C6 to form a bicyclic lactone; and (4) a 1,5 S_N2'' addition of nucleophiles to C2 via a Mg^{2+}-bound transition state.[17] We now demonstrate that ADCS employs an active site nucleophile, K274, that adds to C2 in a S_N2'' reaction. A unifying mechanism for AS, ADCS, and IS is proposed in which all three enzymes initiate their

reactions by addition of either nitrogen or oxygen nucleophiles to C2 of chorismate. Thereafter, the reactions diverge to produce their different products, with AS eliminating pyruvate, ADCS catalyzing a second S_N2'' displacement, and IS simply releasing product.

Materials and Methods

Materials. Chorismic acid (barium salt), PABA, anthranilic acid, NADH, lactate dehydrogenase (LDH), Bicine, DTT, isopropyl-β-D-thiogalactopyranoside (IPTG), pyridoxal 5′-phosphate (PLP) were from Sigma. All other reagents used were analytical grade. Restriction enzymes, DNA ligase, and Vent DNA polymerase were from New England Biolab. Taq DNA polymerase was from Promega. Primers were synthesized by Invitrogen. Synthetic routes to the inhibitors **3**, **12-O**, and **12-N** have been described.[19,20]

Cloning of *pab* Genes. The *pabA, pabB*, and *pabC* genes encoding amidotransferase, ADCS, and ADCL, respectively, were amplified from *Escherichia coli* K12 chromosomal DNA. The primers used for PCR were designed to introduce *Nde*I and *Bam*HI restriction sites into the PCR products. Their sequences are: *pabA*, 5′-TGTACCGGAGCCCA-TATGATCCTGCTT-3′ (forward) and 5′-AATGGATCCCAGAAAT-CAGCGATGCAGGAA-3′ (reverse); *pabB*, 5′-CCAGTAGAGTCAG-GACATATGAAGA-3′ (forward) and 5′-GTATTCCGGATCCTACT-TCTCCAGTTGCTT-3′ (reverse); *pabC*, 5′-CTCTGATAAGGAG-CCCATATGTTC-3′ (forward) and 5′-CTTGGATCCTGACTAAT-TCGGGCGCTCA-3′ (reverse). PCR products from reactions using Vent DNA polymerase were subsequently incubated with Taq DNA polymerase and cloned into the pCR2.1 TA-vector from Invitrogen. Clones containing inserts were isolated by blue-white screening and subcloned into the pET3a vector (Novagen) using the *Nde*I and *Bam*HI restriction sites. The *pabB* and *pabC* genes were subsequently subcloned using the *Nde*I and *Bam*HI restriction sites into the pET28a vector (Novagen) for expression as a 6×His-tagged fusion.

Mutations were introduced into the pET28a-*pabB* construct using the QuikChange Site-Directed Mutagenesis Kit (Stratagene). The

(14) Morollo, A. A.; Finn, M. G.; Bauerle, R. *J. Am. Chem. Soc.* **1993**, *115*, 816−817.
(15) Ye, Q. Z.; Liu, J.; Walsh, C. T. *Proc. Natl. Acad. Sci. U.S.A.* **1990**, *87*, 9391−5.
(16) Anderson, K. S.; Kati, W. M.; Ye, Q. Z.; Liu, J.; Walsh, C. T.; Benesi, A. J.; Johnson, K. A. *J. Am. Chem. Soc.* **1991**, *113*, 3198−3200.
(17) Walsh, C. T.; Liu, J.; Rusnak, F.; Sakaitani, M. *Chem. Rev.* **1990**, *90*, 1105−1129.

(18) Green, J. M.; Nichols, B. P. *J. Biol. Chem.* **1991**, *266*, 12971−5.
(19) Stigers, K. D.; Mar-Tang, R.; Bartlett, P. A. *J. Org. Chem.* **1999**, *64*, 8409−8410.
(20) Kozlowski, M. C.; Tom, N. J.; Seto, C. T.; Sefler, A. M.; Bartlett, P. A. *J. Am. Chem. Soc.* **1995**, *117*, 2128−2140.

K274A primers were: 5′-CCAGACCCGCCCGATTGCAGGCACGC-TACCACGCC-3′ (forward) and 5′-GGCGTGGTAGCGTGCCTGCA-ATCGGGCGGGTCTGG-3′ (reverse) The primers for K274R were: 5′-CCAGACCCGCCCGATTAGAGGCACGCTACCACGCC-3′ (forward) and 5′-GGCGTGGTAGCGTGCCTCTAATCGGGCGGGTCTGG-3′ (reverse).

Overexpression and Purification of PabA (Amidotransferase). *E. coli* BL21 (DE3) Gold cells harboring the pET3a-*pabA* construct were incubated in TB media at 37 °C until the OD_{600} reached 0.5. IPTG was added to 0.5 mM, and the incubation was continued for another 2 h. Cells were harvested by centrifugation and resuspended in lysis buffer (100 mM TEA, pH 7.8, 30 mM β-mercaptoethanol, 1 mM EDTA, 0.5 mg/mL lysozyme, 0.2 units/mL DNase I). The cells were chilled on ice for 15 min and then disrupted by sonication. The following steps were carried out at 4 °C. Cell debris was pelleted by centrifugation at 15,000 rpm for 45 min. The lysate was fractionated with ammonium sulfate (15−40%). The 40% precipitate was dissolved in a minimum volume of starting buffer (50 mM TEA, pH 7.8, 10 mM β-mercapto-ethanol, 5 mM $MgCl_2$, 1 mM EDTA) and loaded onto a ∼75 mL Q-Sepharose Fast Flow column (Pharmacia). The column was washed with 1 bed volume of starting buffer. Proteins were eluted with a linear 0.5-L gradient of 0−300 mM KCl in starting buffer. Fractions were assayed by activity using ADCS and ADCL that were previously purified (see below). Active fractions were pooled, concentrated by ultrafiltration, and dialyzed against 20 mM KP_i, pH 7.4, 50 mM KCl, 1 mM DTT. The final sample was flash-frozen and stored at −80 °C. Protein concentration was determined with the Bio-Rad Dc assay, using IgG as standard. The yield was ∼11 mg purified protein/4 g of cell paste.

Overexpression and Purification of ADCS. TB media was used to culture *E. coli* BL21 (DE3) Gold cells harboring the pET28a-*pabB* construct at 37 °C. Overproduction of ADCS was induced by addition of IPTG to 0.5 mM at OD_{600} = 0.5. Incubation continued for an additional 6−8 h. The cells were harvested, and the pellet was resuspended in starting buffer (20 mM Na_2HPO_4, 500 mM NaCl, 10 mM imidazole, 1 mM β-mercaptoethanol, 0.5 mg/mL lysozyme, 0.2 units/mL DNase I). Cells were chilled on ice and disrupted by sonication. Cell debris was pelleted by centrifugation at 15000 rpm for 45 min. The supernatant was incubated at room temperature for 30 min with Chelating Sepharose Fast Flow resin (Pharmacia) that was charged with Ni^{2+}. The resin was loaded into a column and washed with 15 bed volumes of starting buffer. Bound protein was eluted with a linear 0.5 L 10−300 mM imidazole gradient in 20 mM Na_2HPO_4, 500 mM NaCl, 1 mM β-mercaptoethanol. Activity was determined with the LDH assay (below) using ADCL purified previously. Active fractions were pooled, concentrated, and analyzed by SDS-PAGE. The final protein sample was dialyzed against 20 mM KP_i, pH 7.4, 50 mM KCl, 1 mM DTT, and stored at −80 °C. The overall yield was ∼185 mg ADCS/ 5 g of cell paste.

Overexpression and Purification of ADCL. BL21 (DE3) Gold cells harboring the pET28a-*pabC* construct were grown in 500 mL of TB media that was inoculated with a single colony. The culture was incubated at 30 °C and 200 rpm overnight, and IPTG was added to 0.5 mM when the OD_{600} reached 6−7. Cells were allowed to grow at room temperature and 250 rpm for an additional 16 h after induction. Cells were harvested, and the pellet was resuspended in starting buffer (20 mM Na_2HPO_4, 500 mM NaCl, 10 mM imidazole, 20 μM PLP, 0.5 mg/mL lysozyme, and 0.2 units/mL DNase I). The cells were lysed and loaded onto the nickel resin as for ADCS. It was eluted with a linear 0.5 L 10−350 mM imidazole gradient in 20 mM Na_2HPO_4, 500 mM NaCl, 20 μM PLP. The enzyme was located by its yellow color and its identity confirmed by SDS-PAGE. After dialysis against 20 mM KP_i, pH 7.4, 50 mM KCl, 20 μM PLP, the final sample was stored at −80 °C. The yield was ∼280 mg protein/ 16 g of cell paste.

Spectrophotometric Activity Assays. Enzyme assays were based on previously described methods.[12,15] The first assay employs fluores-
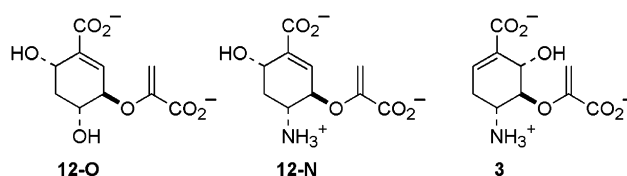
Figure 2. Structures of three potential transition-state analogues for the reaction catalyzed by ADCS.

Table 1. Inhibition Data for ADCS and the K274A Mutant

| enzyme	3		12-O	12-N
	K_i (μM)	K_M/K_i	K_i (μM)	K_i (μM)
ADCS	5.6 ± 0.8	3.4	>1000	>500
K274A	0.7 ± 0.1	83		

cence detection of PABA (excitation at 290 nm, emission at 340 nm) extracted from reaction mixtures containing ADCL as a coupling enzyme and was used for reactions in which the enzyme activity was low. The second directly monitors the formation of PABA by absorbance at 278 nm ($\Delta\epsilon$ = 12340 M^{-1} cm^{-1}) in the ADCL coupled reaction. The third couples pyruvate formation in the ADCL reaction to the LDH reaction, monitoring the decrease in NADH absorbance at 340 nm. The standard glutamine-dependent assay contains 100 mM Bicine, pH 8.5, 20 mM glutamine, 5 mM $MgCl_2$, 20 μM PLP, 13 μM ADCL, 200 μM NADH, 4 units/mL LDH, and equimolar ADCS and PabA. The standard NH_4^+-dependent assay contains 100 mM Bicine, pH 8.5, 100 mM $(NH_4)_2SO_4$, 5 mM $MgCl_2$, 20 μM PLP, 13 μM ADCL, 200 μM NADH, and 4 units/mL LDH. All assays were performed at 25 °C.

HPLC Analysis. HPLC was performed according to a literature procedure.[18] A standard reaction mixture for HPLC analysis contains 100 mM Bicine, pH 8.5, either 20 mM glutamine or 100 mM $(NH_4)_2SO_4$, 5 mM $MgCl_2$, 20 μM PLP, 10 mM chorismate, and 30 μM enzyme(s). After 4 h at room temperature, the pH was lowered to 4, the samples were ultrafiltered to remove protein(s), and injected onto the HPLC. A 5 μm Alltech Alltima (4.6 mm × 150 mm) column was used to separate reaction mixtures on an Agilent 1100 HPLC system. Isocratic elution with 5% acetic acid in water was employed, and the absorbance at 280 nm was monitored. Peaks were identified by comparing retention times and UV absorption spectra with authentic standards.

Identification of Reaction Intermediates. Mass spectral analyses were performed on a Hewlett-Packard 1100 MSD ESI mass spectrometer. Positive ions were detected. The parameter setup was: gain, 10; fragmentor voltage, 40 V; capillary voltage, 3500 V; drying gas flow, 10 L/min; nebulizer pressure, 25 psig; drying gas temperature, 350 °C. The optimum solvent for analyte ionization is 5% acetic acid, which is also the main source of noise. Basic hydrolysis was carried out by heating the sample at 85 °C for 6 h in 1 M NaOH.

Results

Inhibition by 3, 12-O, and 12-N. Compounds **12-O** and **12-N** (Figure 2) were tested as inhibitors of ADCS, and the results are presented in Table 1 and Figure 3. Both compounds are poor, apparently competitive, inhibitors of ADCS with K_i values in the millimolar range. Compound **3** was previously shown to be an inhibitor ($K_i \approx 40$ μM) of ADCS.[20] We repeated this determination with ADCS and extended it to the K274A mutant enzyme. The plots shown in Figure 3 indicate competitive inhibition for both ADCS and K274A. The K_i values obtained are given in Table 1. The difference in the K_i measured previously[20] and that reported here is likely due to differences in buffer conditions (e.g. presence or absence of DTT) and the
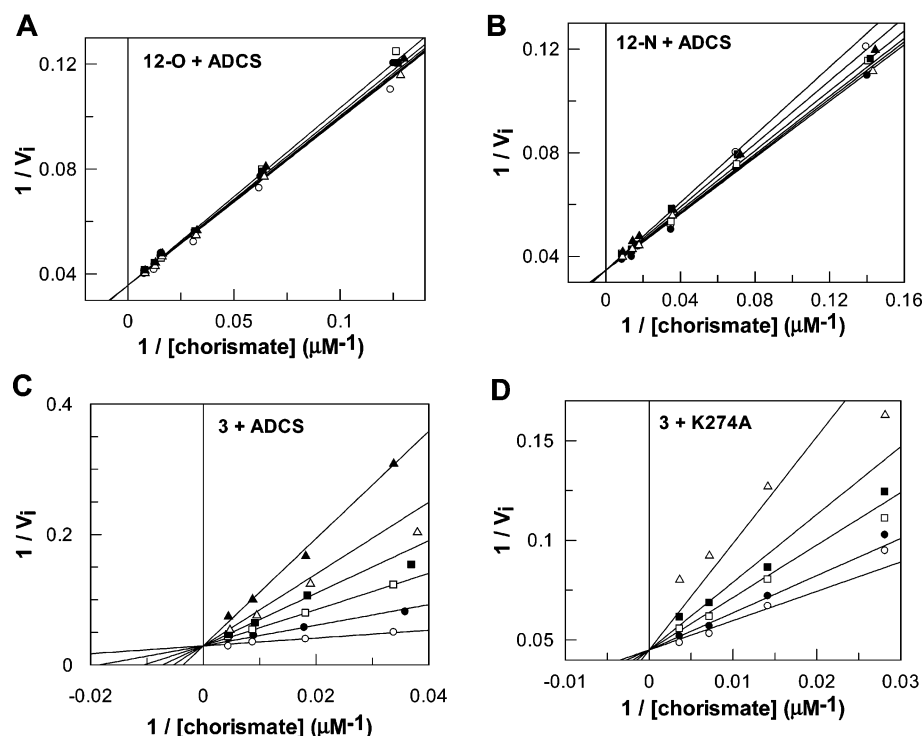
Figure 3. Double reciprocal plots for kinetic analysis of the three potential transition state analogues. The ammonia source was 50 mM ammonium sulfate. (A) Inhibition of ADCS by compound **12-O**. The concentrations of **12-O** were 0 (○), 5 (●), 10 (□), 20 (■), 40 (△), and 78 μM (▲). (B) Inhibition of ADCS by compound **12-N**. The concentrations of **12-N** were 0 (○), 7 (●), 14 (□), 31 (■), 60 (△), and 100 μM (▲). (C) Inhibition of ADCS by **3**. The concentrations of **3** were 0 (○), 9 (●), 21 (□), 33 (■), 47 (△), and 73 μM (▲). (D) Inhibition of K274A by **3**. The concentrations of **3** were 0 (○), 0.2 (●), 0.6 (□), 0.9 (■), and 1.9 μM (△).

use of PabA + glutamine or NH_4^+ as the nitrogen source. The K274A mutant enzyme binds **3** ∼10-fold more tightly than does ADCS. More importantly, the ratio of K_M for chorismate to K_i for **3** is 24-fold higher for K274A.

Active Site Model with Chorismate. The known X-ray structures of ADCS[12] and AS with benzoate and pyruvate bound[9] were employed. A model of chorismate was modeled by hand onto the benzoate and pyruvate ligands of the AS structure, maximizing overlap of the rings and carboxylate groups. The chorismate-containing AS structure was then least-squares superimposed on the ADCS structure using SwissPDB Viewer.[21] The resulting structural overlay is presented as Figure 4.

Steady-State Kinetic Analysis. Steady-state kinetic parameters for ADCS and its K274A and K274R mutants are presented in Table 2. The k_{cat} and K_M values for ADCS with both PabA + glutamine and NH_4^+ as nitrogen sources are in agreement with values reported previously.[5,16] The k_{cat} value for ADCS is 16-fold larger with PabA + glutamine as a nitrogen source than with NH_4^+. The k_{cat} value for the K274A mutant is 265-fold smaller than ADCS with PabA + glutamine as nitrogen source. When 200 mM NH_4^+ is used as the nitrogen source, k_{cat} for K274A increases 13-fold compared to that with PabA + glutamine. This result is in contrast to the behavior of ADCS, which has a lower k_{cat} value with NH_4^+ as a nitrogen source. For ADCS and K274A, the k_{cat} values with saturating NH_4^+ and chorismate are *identical*, and the chorismate K_M values with 200 mM NH_4^+ are similar. The K274R mutant has a k_{cat} value that is 640-fold lower than ADCS using PabA + glutamine. Similar to ADCS and in contrast to K274A, the value of k_{cat}

(21) Guex, N.; Peitsch, M. C. *Electrophoresis* **1997**, *18*, 2714−23.
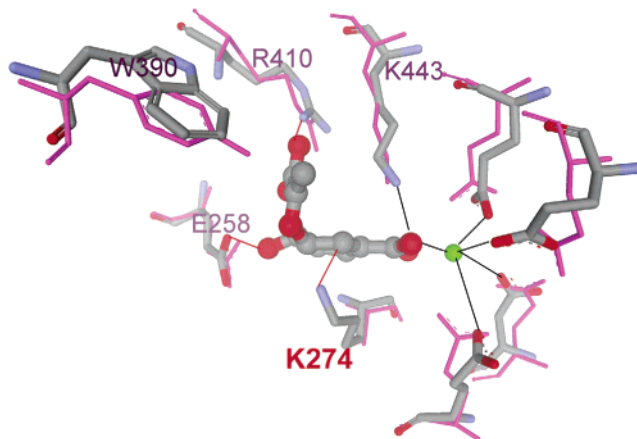
Figure 4. Overlay of the X-ray crystallographic structures of ADCS and AS. The purple structure is that of AS, while ADCS is shown in CPK colors. The green atom is Mg^{2+}. The residue numbers given correspond to the ADCS structure. Chorismate is the molecule docked in the center.

for K274R decreases 8.5-fold when 200 mM NH_4^+ is substituted for PabA + glutamine.

HPLC Analysis of Reactions. The results of the steady-state kinetic analysis described above suggest that NH_4^+ may functionally replace K274 in the K274A mutant, potentially leading to novel reaction products. Thus, the reaction mixtures were subjected to chromatographic separation to identify the products formed in the reactions (Figure 5). The minor peaks observed at ∼8 and ∼10 min in all of the HPLC traces were also present in a control reaction, in which chorismate was incubated in the absence of enzymes, and were not identified. As expected, the reaction of ADCS with chorismate in the presence of NH_4^+ generates a single product, ADC (Figure 5A).

Table 2. Steady-State Kinetic Constants for Chorismate[a]

	ADCS		K274A		K274R
ammonia source	K_M (μM)	k_{cat} (s^{-1})	K_M (μM)	k_{cat} (s^{-1})	k_{cat} (s^{-1})
PabA+Gln	13 ± 1	0.53 ± 0.02		$(2.0 \pm 0.1) \times 10^{-3}$ [b,c]	$(8.3 \pm 0.1) \times 10^{-4}$ [b]
200 mM NH$_4^+$	58 ± 8	0.032 ± 0.002	97 ± 9	0.026 ± 0.001	$(9.8 \pm 0.9) \times 10^{-5}$ [b]

[a] Standard reaction conditions given under Material and Methods were used throughout. The values of K_M for NH$_4^+$ for ADCS and K274A are 145 ± 36 and 169 ± 12 mM, respectively. The k_{cat} values obtained from NH$_4^+$ saturation curves with a constant, saturating chorismate concentration are 0.032 ± 0.003 and 0.033 ± 0.001 s^{-1}, respectively, for the two enzymes. These values were measured using the PABA absorbance assay. [b] Data were determined using the end-point fluorescence assay due to the slow nature of the reactions. Saturating chorismate (1 mM) was used and K_M values were not determined. All other values were determined using the LDH assay. [c] The reaction of K274A in the presence of PabA+glutamine+200 mM NH$_4^+$ as nitrogen sources gives a k_{cat} value of 0.010 ± 0.001 s^{-1}, 5-fold higher than in the absence of NH$_4^+$.
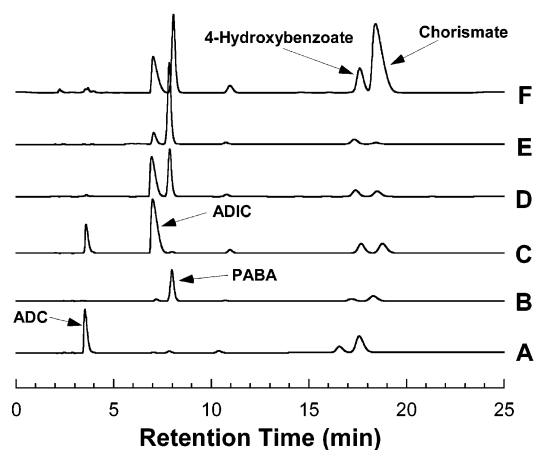

Figure 5. HPLC fractionation of ADCS and K274A reaction mixtures. (A) ADCS + NH$_4^+$. (B) Reaction mixture A incubated with ADCL for 20 min. (C) K274A + NH$_4^+$. (D) Reaction mixture C incubated with ADCL after K274A had been removed. (E) Reaction C incubated with ADCL without removing K274A. (F) K274A + PabA + Gln. The PABA produced in this reaction is due to trace contamination of the PabA preparation with ADCL. The small variation in chorismate retention time is due to slightly different chromatographic conditions on different dates. Standards were run on each date to confirm identities.

Chemical identification of this peak is presented below. When ADCL is added to this reaction mixture, the ADC is completely converted to PABA, also as expected (Figure 5B).

In contrast, the reaction of K274A in the presence of NH$_4^+$ generates two peaks, ADC and ADIC, with the chemical identification of the latter also presented below. The time dependence of the K274A reaction shows that the equilibrium mixture (shown in Figure 5C) has a molar ratio of ~1.6:1 for ADIC and ADC, respectively. When K274A is removed from this reaction mixture by ultrafiltration and ADCL is subsequently added, the ADC peak is converted to a PABA peak and the ADIC peak remains unchanged (Figure 5D). If K274A is not removed before adding ADCL, both the ADC and the ADIC peaks are converted to a PABA peak due to the reversible nature of the ADC/ADIC interconversion (Figure 5E). Finally, when PabA + glutamine is used as the nitrogen source with K274A the formation of ADIC is observed, as is PABA and a small amount of ADC (Figure 5F). The formation of PABA in this reaction has been shown to be due to contamination of the PabA preparation with a small amount of ADCL (He and Toney, unpublished results).

Identification of ADC and ADIC. The peaks in the HPLC traces that were expected to be ADC and ADIC based on enzymatic activities and lack of correspondence to standards were identified chemically. Figure 6 presents both mass spectral and hydrolytic analyses. The putatitve ADC and ADIC peaks
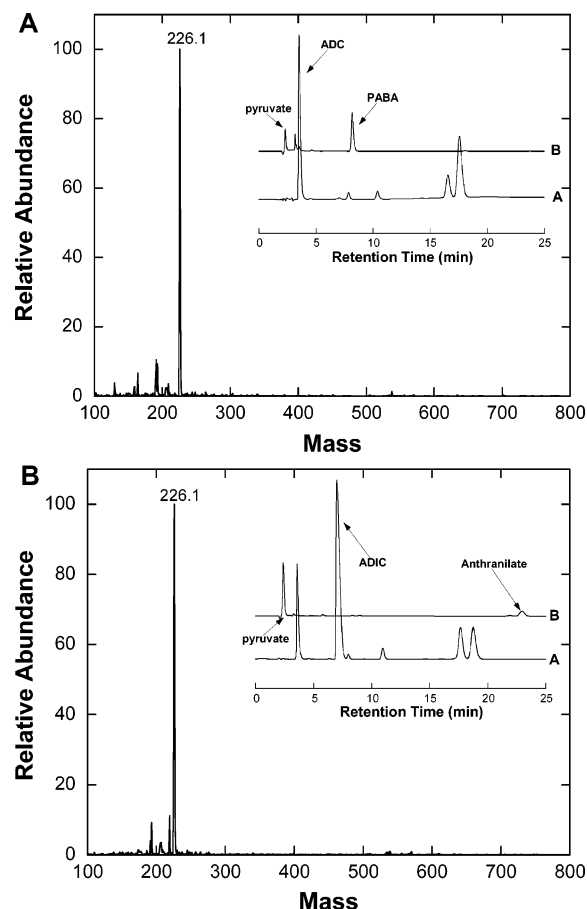
Figure 6. Chemical identification of ADC and ADIC by mass spectral analysis and basic hydrolysis. (A) ADC. (B) ADIC. The calculated molecular weights of both ADC and ADIC are 226.07 amu. (Inset) HPLC chromatograms of basic hydrolysis reactions. Traces A and B are, respectively, for the reactions mixtures from which the samples (labeled) were collected, and for the samples after hydrolysis.

were collected from the HPLC from ADCS and K274A reactions, respectively. The mass spectrum of the assumed ADC peak is shown in Figure 6A. The observed mass of 226.1 corresponds well to the predicted mass of 226.07 amu for the cationic form of ADC. The inset shows HPLC traces for the ADCS reaction from which the ADC peak was collected (A) and the sample after hydrolysis (B). PABA and pyruvate are the observed products, as expected for ADC hydrolysis. The mass spectrum of the ADIC peak is shown in Figure 6B; again, the observed mass corresponds to that predicted for ADIC. The inset shows HPLC traces of the K274A reaction from which the ADIC peak was collected (A) and the sample after hydrolysis (B). Anthranilate and pyruvate are the observed products, as expected for ADIC hydrolysis. The possibility that the proposed
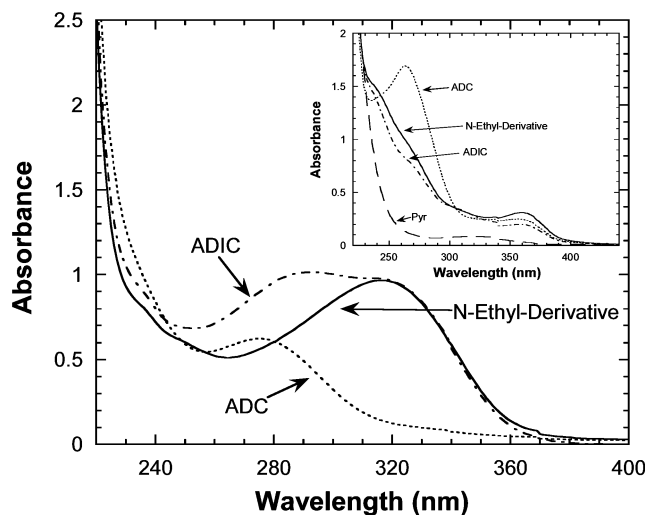
Figure 7. Spectral identification of the *N*-ethyl derivative of aminodeoxy-chorismate formed in the reaction of K274A with ethylamine. (A) UV spectra of the *N*-ethyl derivative, ADIC, and ADC before basic hydrolysis. (B) UV spectra of the *N*-ethyl derivative, ADIC, and ADC after basic hydrolysis, performed by incubation in 1 M NaOH at 85 °C for 6 h.

ADIC peak in the HPLC trace is the C6 adduct of ammonia to chorismate is ruled out by the UV spectroscopic properties of the intermediate. The data presented in Figure 7 show long wavelength absorption that would be absent from the C6 adduct due to the loss of conjugation between the double bonds in the ring. Additionally, the C6 hydroxyl adduct has been synthesized and shown to be unstable under these conditions.[22] The spectral properties of the collected peaks (Figure 7), both before and after hydrolysis, are highly consistent with their assignments as ADC and ADIC.

Identification of the *N*-Ethyl Derivative Formed in K274A Reactions with Ethylamine. The use of 200 mM ethylamine as the only amine (i.e. no source of NH_4^+) in K274A reactions produced a new peak at 10.6 min in the HPLC traces (data not shown). This peak was collected and identified by its mass spectrum and absorbance. The observed mass of 253.9 is in good agreement with the predicted value of 254.1 amu. Figure 7 shows the absorption spectrum of the *N*-ethyl derivative in comparison to those of ADIC and ADC. The *N*-ethyl derivative shows a ~320 nm band that is characteristic of ADIC. The inset shows spectra of the same compounds after basic hydrolysis. The ADC sample produces PABA with its characteristic ~275 nm peak. Both the *N*-ethyl derivative and ADIC give spectra lacking this band. This mass and UV/vis spectral evidence strongly supports the structure of the *N*-ethyl derivative as that of *N*-ethyl-ADIC.

Discussion

The similiarities in the reactions catalyzed by AS, ADCS, and IS, as well as their sequence homologies, have inspired a search for a unifying mechanism for these three enzymes. Walsh et al.[17] proposed three possible unifying mechanisms by which the transformations could occur: (1) addition of an enzyme nucleophile to C6 of chorismate in an S_N2' fashion, followed by a second S_N2' displacement of the enzyme nucleophile, (2) addition of the substrate enolpyruvyl side chain carboxylate to C6 to form a bicyclic lactone followed by a second S_N2'

(22) Mattia, K. M.; Ganem, B. *J. Org. Chem.* **1994**, *59*, 720−728.

displacement, and (3) concerted S_N2'' displacement involving C2 addition/C4 substitution through a Mg^{2+}-bound transition state. A fourth possibility, Michael addition at C2 followed by elimination at C4, was considered for AS and IS but was discounted as a mechanism for introducing the C4 amino group in ADCS.

Walsh et al.[23] synthesized three analogues of chorismate with electrophilic groups at C6, none of which trapped an enzyme nucleophile. This result weighs against the first mechanistic possibility above. Kozlowski et al.[20] synthesized three potential analogues for the concerted Mg^{2+}-bound transition state. They found these compounds to be good inhibitors of AS and IS but only weak inhibitors of ADCS. Thus, it was considered that ADCS might employ a concerted Mg^+-bound transition state involving S_N2' addition of an exogenous nucleophile (e.g., H_2O) to C6 instead of C2 in a first step, followed by a second S_N2' step in which NH_3 adds to C4. The compounds **12-O** and **12-N** (Figure 2) were synthesized to probe this possibility.[19] The data presented in Figure 3 and summarized in Table 1 show that both of these compounds are very poor inhibitors of ADCS. These results, and those from Walsh's earlier studies, argue strongly against a mechanism for ADCS in which a nucleophile is added to C6.

The possible mechanisms for ADCS were reevaluated in this light. The fourth mechanism mentioned above, Michael addition at C2 with S_N2'' displacement at C4 could, in principle, be followed by all three enzymes if ADCS employs an active site nucleophile at C2, instead of NH_3 or H_2O like AS and IS. The ADCS reaction would then be completed by a second S_N2'' displacement of the enzyme nucleophile at C2 by addition of NH_3 at C4. This mechanism would also explain the relatively poor inhibition of ADCS observed for analogues of the transition state for C2/C4 concerted displacement, since the enzyme nucleophile would interfere sterically with the inhibitor's C2 substituent.

The structures of AS and ADCS have been solved crystallographically.[9−12] The benzoate-bound AS structure[9] was used as a template for modeling the interaction of chorismate in the active site. This AS-chorismate model was then least-squares superimposed on the structure of ADCS[12] to generate the overlay used for Figure 4. The most striking feature of this overlay is the close positioning of the ϵ-amino group of K274 in ADCS to C2 of chorismate, in good orientation to add to C2 in an S_N2'' process that would generate a covalent enzyme intermediate. In AS and IS, the structurally homologous position is strictly conserved as an alanine (He and Toney, unpublished results).

The hypothesis that K274 addition to C2 of chorismate initiates the ADCS reaction was tested by analyzing the K274A and K274R active site mutants. When PabA + glutamine are used as the nitrogen source, both mutant enzymes have greatly reduced k_{cat} values (265 and 640-fold, respectively), which supports the proposal that K274 participates as a nucleophile in the reaction. The reactions of the mutant enzymes with 200 mM NH_4^+ as the nitrogen source gave surprising and remarkable results. The k_{cat} value of the K274A mutant *increases* 13-fold while that of the K274R mutant *decreases* 8.5-fold. The decrease in k_{cat} for the K274R mutant when 200 mM NH_4^+ is used as the nitrogen source is similar to that seen with ADCS (16-fold). The binding of PabA to ADCS likely induces conformational changes in the ADCS active site that activate it for catalysis.

The increase in k_{cat} for the K274A mutant on switching from PabA + glutamine to NH_4^+ as the nitrogen source strongly suggests that NH_4^+ is playing a more significant role in this mutant than simply that of a cosubstrate. We hypothesized that NH_4^+ assumes the role of the missing K274 functional group by adding to C2 in a chemical rescue, forming ADIC as a noncovalently bound intermediate in place of the K274-linked adduct in the normal process. This hypothesis is supported by the observation that the k_{cat} values of ADCS and K274A are *identical* under conditions of saturating NH_4^+ and chorismate, in the absence of PabA (Table 2). This identity of k_{cat} values would occur if NH_4^+-assisted catalysis is effective to the point that nucleophilic addition at C2 is not rate-limiting, and the mutant and wild type have a common rate-limiting step (e.g., product release).

Direct evidence for formation of ADIC in the course of the K274A-catalyzed reaction, but not that of ADCS, was obtained by HPLC analysis (Figure 5). The reaction catalyzed by ADCS using NH_4^+ as the nitrogen source shows the production of ADC as the sole product. When ADCL is added to this reaction, the ADC formed is converted to PABA, as expected. If NH_4^+ is functionally replacing K274 in the K274A mutant, as proposed above, ADIC would accumulate in the reaction mixture if the rate of release of ADIC is comparable to the rate of addition of a second molecule of NH_4^+ at C4 to give ADC. This expectation was confirmed by the appearance of *both* ADC and ADIC in the K274A-catalyzed reaction with NH_4^+ as the nitrogen source (Figure 5C). The ADIC formed in the K274A reaction is in enzyme-catalyzed equilibrium with ADC, hence all is carried on to PABA in the presence of ADCL (Figures 5D and E).

The use of PabA + glutamine as nitrogen source for the K274A mutant also leads to the formation of ADIC (Figure 5F), demonstrating that the NH_3 generated by PabA in complex with ADCS can indeed add to C2, as occurs in the analogous reaction of AS. Although the efficiency with which NH_3 generated at the PabA active site is channeled into the ADCS active site has not been reported, one expects it to be high based on precedents with, for example, GMP synthetase and CTP synthetase.[24,25] In this regard, it was surprising to find that the K274A reaction with PabA + glutamine *and* 200 mM NH_4^+ as nitrogen source gave a k_{cat} value 5-fold greater than in the absence of NH_4^+ (Table 2, footnote c). The NH_4^+ (or NH_3) apparently gains ready access to the ADCS active site from solvent in the presence PabA, possibly with the exogenous NH_4^+ having greater access to C2 than that generated from PabA + glutamine.

In contrast to the ease with which NH_3 gains access to the active site and adds to the C2 and C4 positions, water apparently does not, since no isochorismate is observed in the K274A reaction with either PabA + glutamine or NH_4^+ as nitrogen source. This result is somewhat surprising given that (1) the structurally homologous residue to K274 in IS is an alanine, (2) IS employs water as the nucleophile at C2, and (3) IS has been shown to add NH_3 to C2 of chorismate (20). The structural basis of the discrimination between nitrogen and oxygen nucleophiles in the addition to C2 of chorismate remains to be explained.
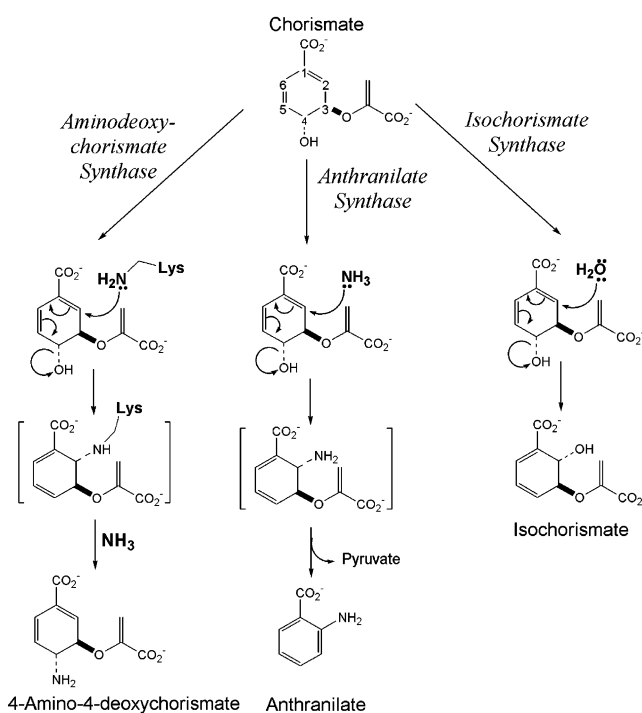
Figure 8. Conservation of mechanism among the three homologous chorismate utilizing enzymes AS, ADCS, and IS. The ring carbon numbers are shown for chorismate. All three enzymes initiate their reactions by addition of either a nitrogen or an oxygen nucleophile to C2, with either concerted or stepwise elimination of hydroxide from C4. AS and IS both employ exogenous nucleophiles, while ADCS uses the ϵ-amino group of K274.

The inclusion of 200 mM ethylamine in the reactions of K274A using either PabA + glutamine or NH_4^+ as the nitrogen source does not increase the reaction rate. This result was surprising in view of the examples in the literature of alkylamine rescue of lysine mutants of other enzymes.[26-28] A simpler experiment was thus attempted: using ethylamine as the only nitrogen source produced a new peak in the HPLC trace that was identified as *N*-ethyl-ADIC by mass and UV spectroscopies.

The findings that ADIC is formed in the K274A reactions with either NH_4^+ or PabA + glutamine as the nitrogen source, and that ethylamine can also function as a C2 nucleophile in this mutant, strongly implicate K274 as an active site nucleophile that initiates the ADCS reaction by adding to C2 of chorismate. Additionally, this proposal is supported by the inhibition results with **3** and with **12-O** and **12-N**. It is clear why the latter two analogues, which mimic the transition state for a concerted 6,4 S_N2' displacement, are ineffective as inhibitors of ADCS. That **3**, which is so potent against IS and AS, is weaker against ADCS is consistent with adverse steric interactions between the hydroxyl group of **3** and the side chain of K274 in ADCS. This interpretation is supported by the observation that the ratio of K_M for chorismate to K_i for **3** is only 3.4 for ADCS but increases to 83 with the K274A mutant, in which this steric interaction is relieved.

Figure 8 presents a unifying core mechanism for AS, ADCS, and IS. In all three enzymes, the reactions are initiated by addition of a nucleophile to C2 of chorismate in an S_N2''

(23) Walsh, C. T.; Erion, M. D.; Walts, A. E.; Delany, J. J., III; Berchtold, G. A. *Biochemistry* **1987**, *26*, 4734−45.
(24) Zalkin, H.; Truitt, C. D. *J. Biol. Chem.* **1977**, *252*, 5431−6.
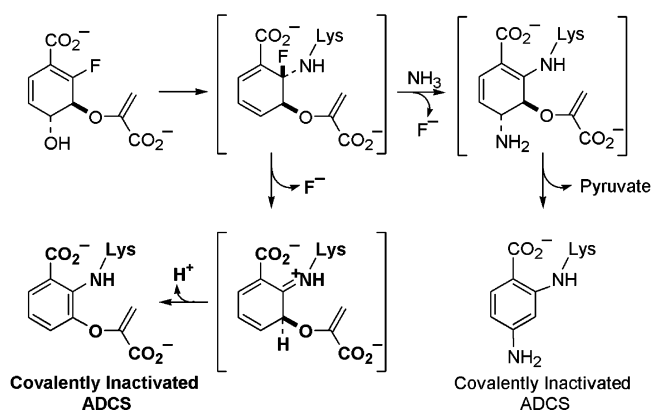(25) Levitzki, A.; Koshland, D. E., Jr. *Biochemistry* **1971**, *10*, 3365−71.

(26) Toney, M. D.,; Kirsch, J. F. *Science* **1989**, *243*, 1485−8.
(27) Harpel, M. R.; Hartman, F. C. *Biochemistry* **1994**, *33*, 5553−61.
(28) Jiang, W.; Locke, G.; Harpel, M. R.; Copeland, R. A.; Marcinkeviciene, J. *Biochemistry* **2000**, *39*, 7990−7.

mechanism, with concomitant loss of the hydroxyl group at C4. The AS reaction forms ADIC as a tightly bound intermediate that reacts further by elimination of the enolpyruvoyl moiety to give anthranilate. IS simply adds H_2O (or OH^-) to C2 and releases product. ADCS adds the ϵ-amino group of K274 to C2 to form a covalent intermediate. A second S_N2'' addition of NH_3 at C4 with concomitant loss of K274 at C2 affords the final product, ADC.

The ADCS mechanism involving covalent attachment of the substrate through K274 provides clear directions for the design of inhibitors, as well as a rationale for the anti-bacterial properties of (6*S*)-6-fluoroshikimate.[29,30] Sequential processing of this derivative by shikimate kinase, EPSP synthase, and chorismate synthase affords 2-fluorochorismate, which is expected to undergo ready S_N2'' displacement by K274 in the active site of ADCS (Figure 9). The covalent intermediate formed can react by two possible pathways: (1) direct fluoride loss to form an imine that aromatizes and covalently inactivates ADCS, and (2) addition of ammonia at C4 with loss of fluoride and subsequent pyruvate elimination. We favor the former mechanism (highlighted in bold in Figure 9) since geminal

(29) Bornemann, S.; Ramjee, M. K.; Balasubramanian, S.; Abell, C.; Coggins, J. R.; Lowe, D. J.; Thorneley, R. N. *J. Biol. Chem.* **1995**, *270*, 22811−5.
(30) Davies, G. M.; Barrett-Bee, K. J.; Jude, D. A.; Lehan, M.; Nichols, W. W.; Pinder, P. E.; Thain, J. L.; Watkins, W. J.; Wilson, R. G. *Antimicrob. Agents Chemother.* **1994**, *38*, 403−6.

Figure 9. Mechanism-based inhibition of ADCS by 2-fluorochorismate. The pathway shown in bold is expected to be favored.

fluoride loss from the initial covalent intermediate and subsequent aromatization are expected to be facile, and the pyruvate elimination step required in the alternative mechanism is not catalyzed by ADCS. Thus, while (6*S*)-6-fluoroshikimate is not a reactive molecule or enzyme inhibitor in its own right, it takes advantage of the biosynthetic pathway from shikimate to chorismate to deliver a potent, mechanism-based inhibitor to ADCS.